Journal of Applied Physics

Unidirectional invisibility of an acoustic multilayered medium with parity-time-symmetric impedance modulation

Cite as: J. Appl. Phys. **129**, 175106 (2021); https://doi.org/10.1063/5.0039432
Submitted: 03 December 2020 • Accepted: 16 April 2021 • Published Online: 04 May 2021

Shuowei An, Tuo Liu, Shanjun Liang, et al.

AIP Publishing

Journal of Applied Physics ARTICLE scitation.org/journal/jap

Unidirectional invisibility of an acoustic multilayered medium with parity-time-symmetric impedance modulation

Cite as: J. Appl. Phys. **129**, 175106 (2021); doi: 10.1063/5.0039432
Submitted: 3 December 2020 · Accepted: 16 April 2021 ·
Published Online: 4 May 2021

Shuowei An,[1] Tuo Liu,[1,2,a)] Shanjun Liang,[3] He Gao,[1,2] Zhongming Gu,[1,2] and Jie Zhu[1,2,a)]

AFFILIATIONS

[1]Department of Mechanical Engineering, The Hong Kong Polytechnic University, Hung Hom, Kowloon, Hong Kong SAR, China
[2]The Hong Kong Polytechnic University Shenzhen Research Institute, Shenzhen 518057, People's Republic of China
[3]Division of Science, Engineering and Health Studies, College of Professional and Continuing Education, Hong Kong Polytechnic University, Hung Hom, Kowloon, Hong Kong SAR, China

Note: This paper is part of the Special Topic on Acoustic Metamaterials 2021.
[a)]**Authors to whom correspondence should be addressed**: tuoliu@polyu.edu.hk and jiezhu@polyu.edu.hk

ABSTRACT

Non-Hermitian scattering systems respecting parity-time symmetry exhibit unidirectional invisibility or reflectionlessness at an exceptional point of the scattering matrix. In this study, we investigate the scattering properties of a one-dimensional acoustic parity-time-symmetric multilayered medium. Parity-time symmetry is defined by a spatial small-amplitude square-wave modulation of the medium parameters in the complex plane. Such a multilayered medium has been demonstrated to reach an exceptional point and support unidirectional invisibility for balanced real and imaginary part modulations of the refractive index. Through the analysis of interference within the medium, we show that the complex modulation of acoustic impedance instead of the refractive index governs the exceptional point of the scattering matrix and determines the occurrence of the unidirectional invisibility. This unidirectional invisibility is further investigated for more general cases of complex parameter distribution including unequal modulation amplitudes and rectangular wave modulation. Our study provides an intuitive physical picture of the occurrence of unidirectional invisibility induced by an exceptional point in acoustic wave systems. Moreover, this study could facilitate the design and practical realization of acoustic parity-time-symmetric structures.

I. INTRODUCTION

Parity-time-symmetric (PT-symmetric) systems are a class of non-Hermitian systems whose Hamiltonians commute with the combined PT operator. This type of system experiences a transition from the PT-symmetric phase to the PT-broken phase once the non-Hermitian parameters reach a certain threshold. During this transition, the real eigen-spectrum becomes complex abruptly.[1] The point that connects these two phases is known as the PT-symmetry breaking point or exceptional point (EP), which is associated with many intriguing phenomena and applications.[2–7]

In PT-symmetric scattering systems, EP can induce unidirectional invisibility, that is, reflection vanishes from one side, and transmission occurs as if the structure did not exist.[8] This extraordinary phenomenon was first theoretically predicted in a complex PT-symmetric optical grating having balanced real-part refractive index and gain/loss modulations.[9] A loss-biased passive version of such PT-symmetric potential supporting unidirectional reflectionlessness, which is a more general case of an EP of the scattering matrix, was then demonstrated experimentally through a Si-based optical waveguide with only adsorptive media.[10]

The EP-induced unidirectional invisibility or reflectionlessness, in general, can be mathematically described by the coalescence of eigenvalues of a scattering matrix.[11,12] PT-symmetric or non-Hermitian acoustic scattering systems regarding their practical implementation have mainly two types. The first type used lumped gain and/or loss elements without clear thickness to synthesize EPs of the scattering matrix, for example, via loudspeaker units loaded with active circuits,[13,14] diaphragms within an airflow

duct,[15] and passive resonant structures with asymmetric loss.[16–19] For the second type, which is the focus of this study, EPs of the scattering matrix are achieved by bulk materials with effective parameters spatially modulated in the complex plane following certain patterns.[20–25] Specifically, EP-induced unidirectional invisibility appears in a PT-symmetric periodic medium whose refractive index distribution satisfies a complex exponential modulation or a more practical square-wave modulation.[20,21] In most existing works, this type of complex index distribution is achieved by tuning one of the two material parameters (e.g., bulk modulus) while keeping the other one (e.g., density) unchanged. However, both of the two effective parameters usually alter simultaneously with regard to their experimental realization with artificial materials,[22,26,27] which brings challenges to the overall design. Although several approaches have been proposed to overcome this obstacle, such as, through sidewall structures within acoustic waveguides[20–23,25,27] similar to the acoustic liners,[28,29] still, the stringent requirements inevitably limit their practicability. More importantly, the necessary condition, in terms of material parameter distribution, to access an EP of the scattering matrix and realize the resultant unidirectional invisibility in PT-symmetric media remains unclear.

In this study, we present two examples to show that the unidirectional invisibility supported by an acoustic PT-symmetric refractive index distribution at an EP can take place in the opposite direction or even disappear when the density and modulus are modulated simultaneously. To determine which parameter governs the EP of the scattering matrix, we analyze the interference of backscattered waves and demonstrate that, in the small-modulation regime, the acoustic impedance instead of the refractive index exclusively determines the occurrence of the unidirectional invisibility in the PT-symmetric medium. In addition, the broadband response is investigated in the cases of unequal amplitudes of real and imaginary part modulations and rectangular wave modulation. Our results offer a deeper understanding of EPs in acoustic scattering systems and would benefit the practical design and applications of PT-symmetric or other non-Hermitian acoustic structures under complex small-amplitude modulation.

II. PT-SYMMETRIC MULTILAYERED MEDIUM

The one-dimensional periodic PT-symmetric acoustic medium with N periods is immersed in the background medium, as depicted in Fig. 1(a). The background medium parameter X (X can be density, bulk modulus, refractive index, or acoustic impedance) is modulated by a complex square-wave function $\Delta X(x)$ ($|\Delta X| \ll X$) as shown in Fig. 1(b). In this function, T is the modulation period, l_1 and l_2 are the thicknesses of the negative and positive half cycles of the real part modulation ($T = l_1 + l_2$), m is the duty ratio of the positive real part modulation defined as $m = l_2/T$, and ε and δ are the modulation amplitudes of the real and imaginary parts. Each period is composed of four layers (A, B, C, and D).

The proposed configuration widely employed in the studies of PT-symmetric systems[10,20,21] consists of real and imaginary part modulations, which is different from the pure gain-loss distribution discussed in Ref. 11. Evolved from the continuous complex

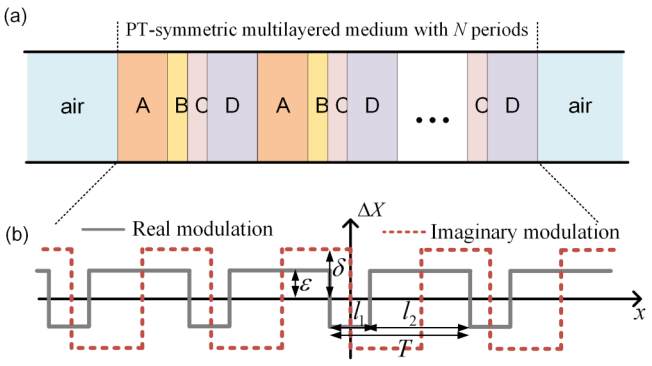

FIG. 1. One-dimensional acoustic medium under PT-symmetric modulation. (a) Schematic of the multilayered periodical medium inserted in the background medium. The medium is composed of four components A, B, C, and D with N periods; (b) parameter ΔX under complex square-wave modulation.

exponential function, this square-wave function configuration is proposed to simplify experimental realization and can be readily implemented by combining sidewall structures and micro-loudspeakers. In detail, the sidewall structures such as micro-perforations and grooves have been proved to mimic homogenous resistive and capacitive boundaries for real-part index and loss modulation, respectively.[20–22] The most challenging part may be to construct a homogenous gain element. Emerging schemes such as virtual atom and loudspeaker units loaded with circuits can serve as potential candidates of gain media.[13,26,30] Achieving the proposed configuration is possible by embedding these micro-loudspeakers array into the sidewall structure, provided that the micro-loudspeakers and their intervals are much smaller than the wavelength.

III. TRANFER MATRIX METHOD

To analyze the scattering properties of the multilayered medium, the transfer matrix method is employed.[31] After omitting the time dependency $e^{i\omega t}$, the one-dimensional linear acoustic wave equation can be expressed as

$$\frac{d^2p(x)}{dx^2} + \frac{\omega^2}{c^2}p(x) = 0, \tag{1}$$

where p, ρ, κ, $c = \sqrt{\kappa/\rho}$, f, and $\omega = 2\pi f$ represent the acoustic pressure, density, modulus, speed of sound, frequency, and angular frequency, respectively. The general solution of the acoustic pressure field subject to Eq. (1) is given by

$$p(x) = P_f e^{-ikx} + P_b e^{ikx}, \tag{2}$$

and the particle velocity is obtained as

$$v(x) = -\frac{1}{i\omega\rho}\frac{\partial p}{\partial x} = \frac{P_f e^{-ikx}}{\rho c} - \frac{P_b e^{ikx}}{\rho c}, \tag{3}$$

where P_f and P_b denote the acoustic pressure of forward and backward propagating waves and k is the wave number. Given the continuity of pressure and normal particle velocity at the interfaces as shown in Fig. 1(a), the sound pressure and normal acoustic particle velocity on two sides of any individual layer can be connected by a 2×2 transfer matrix T_Y,

$$\begin{bmatrix} p(x_M) \\ v(x_M) \end{bmatrix} = T_Y \begin{bmatrix} p(x_N) \\ v(x_N) \end{bmatrix}, \tag{4}$$

where M and N represent two adjacent layers. The transfer matrix T_Y is expressed as

$$T_Y = \begin{bmatrix} \cos(k_Y l_Y) & i\rho_Y c_Y \sin(k_Y l_Y) \\ i\sin(k_Y l_Y)/\rho_Y c_Y & \cos(k_Y l_Y) \end{bmatrix}, \tag{5}$$

where k_Y, l_Y, ρ_Y, and c_Y represent the wavenumber, thickness, density, and speed of sound of layer Y, respectively (Y can be A, B, C, or D). For the PT-symmetric medium with a total number of periods N, the forward and backward transfer matrices of the entire system are expressed as

$$T^f = (T_A \cdot T_B \cdot T_C \cdot T_D)^N, \tag{6a}$$

$$T^b = (T_D \cdot T_C \cdot T_B \cdot T_A)^N. \tag{6b}$$

The overall reflection and transmission coefficients for forward and backward incidences can be obtained from the elements of the transfer matrix as

$$r_{f,b} = \frac{T_{11}^{f,b} + \left(\frac{T_{12}^{f,b}}{\rho_0 c_0}\right) - \rho_0 c_0 T_{21}^{f,b} - T_{22}^{f,b}}{T_{11}^{f,b} + \left(\frac{T_{12}^{f,b}}{\rho_0 c_0}\right) + \rho_0 c_0 T_{21}^{f,b} + T_{22}^{f,b}}, \tag{7a}$$

$$t_{f,b} = \frac{2e^{jk_0 NT}}{T_{11}^{f,b} + \left(\frac{T_{12}^{f,b}}{\rho_0 c_0}\right) + \rho_0 c_0 T_{21}^{f,b} + T_{22}^{f,b}}, \tag{7b}$$

with ρ_0, c_0, and k_0 being the density, sound speed, and wave number, respectively, of the background medium.[31] T is the length of a period of the multilayered medium. Considering the reciprocity, $t_f = t_b = t$.

The entire multilayered medium is immersed in a homogenous background medium (regions outside the multilayered medium) and works as a two-port system that can be fully described by a 2×2 scattering matrix. This matrix connects the pressure amplitudes of forward and backward propagating waves outside the entire multilayered medium,

$$\begin{bmatrix} P_f|_{x\geq\frac{NT}{2}} \\ P_b|_{x\leq\frac{-NT}{2}} \end{bmatrix} = S \begin{bmatrix} P_f|_{x\leq\frac{-NT}{2}} \\ P_b|_{x\geq\frac{NT}{2}} \end{bmatrix}, \quad S = \begin{bmatrix} t & r_b \\ r_f & t \end{bmatrix}. \tag{8}$$

IV. KEY ROLE OF THE ACOUSTIC IMPEDANCE

A. Limitation of the refractive index description

We start from the normal case, that is, the parameter $X + \Delta X$ mentioned in Sec. II represents the refractive index distribution $n + \Delta n$. The modulation is only applied to the bulk modulus (Table I). The reflection and transmission coefficients are calculated using the transfer matrix method. The background medium is air with refractive index $n_0 = 1$, density $\rho_0 = 1.21\ \mathrm{kg/m^3}$, and bulk modulus $\kappa_0 = 0.14236\ \mathrm{MPa}$. The modulation period T is set as 0.06 m with $l_1 = l_2$, and its number N is chosen as a relatively small value, 10 to avoid the breakdown of unidirectional invisibility.[8] The amplitudes of the refractive index modulation, ε_n and δ_n, are both 0.005 that satisfies the small-amplitude modulation.

As shown in Figs. 2(a) and 2(b), the vanishing reflection from the backward direction and the unitary transmission coefficient ($|r_b| = 0$ and $|t| = 1$) are observed at the first Bragg frequency $f_B = c_0/(2T)$, 2858.33 Hz, which satisfies the generalized unitary relation.[11,12] This unidirectional reflectionlessness can be understood from the fact that the square-wave modulation provides a unidirectional modulation vector in momentum space.[20] Intrinsically, this effect takes place at an EP of the scattering matrix defined in the parameter space when $\delta/\varepsilon = 1$, which corresponds to the coalesced and unimodular eigenvalues $\left(\lambda_{1,2} = t \pm \sqrt{r_b r_f}\right)$ with one of the reflection coefficients vanishing [Fig. 2(c)]. Moreover, Fig. 2(b) shows the transmission phase $|\phi_t| = 0$ at f_B. The above three features ($|r_b| = 0$, $|t| = 1$, and $|\phi_t| = 0$) indicate that the multilayered medium is invisible when probed from the backward direction, namely, the so-called unidirectional invisibility phenomenon.

The above refractive index description has been widely used in acoustic PT-symmetric scattering systems.[20–22,25,27] However, this description may no longer work when the two material parameters, ρ and κ, are simultaneously modulated. To demonstrate this point, two counterexamples, cases I and II, are given as follows.

In case I, the refractive index modulation reflects in the bulk moduli of components A and C and the densities of components B and D, as listed in Table II. Notably, the resultant refractive index distribution $n = c_0\sqrt{\rho/\kappa}$ still satisfies the square-wave modulation as given in the normal case. According to the previous experience,

TABLE I. Parameter distribution for the normal case.

Component	A	B	C	D
ρ	ρ_0	ρ_0	ρ_0	ρ_0
κ	$\frac{\kappa_0}{(1+\varepsilon+\delta i)^2}$	$\frac{\kappa_0}{(1-\varepsilon+\delta i)^2}$	$\frac{\kappa_0}{(1-\varepsilon-\delta i)^2}$	$\frac{\kappa_0}{(1+\varepsilon-\delta i)^2}$
n	$n_0(1+\varepsilon+\delta i)$	$n_0(1-\varepsilon+\delta i)$	$n_0(1-\varepsilon-\delta i)$	$n_0(1+\varepsilon-\delta i)$

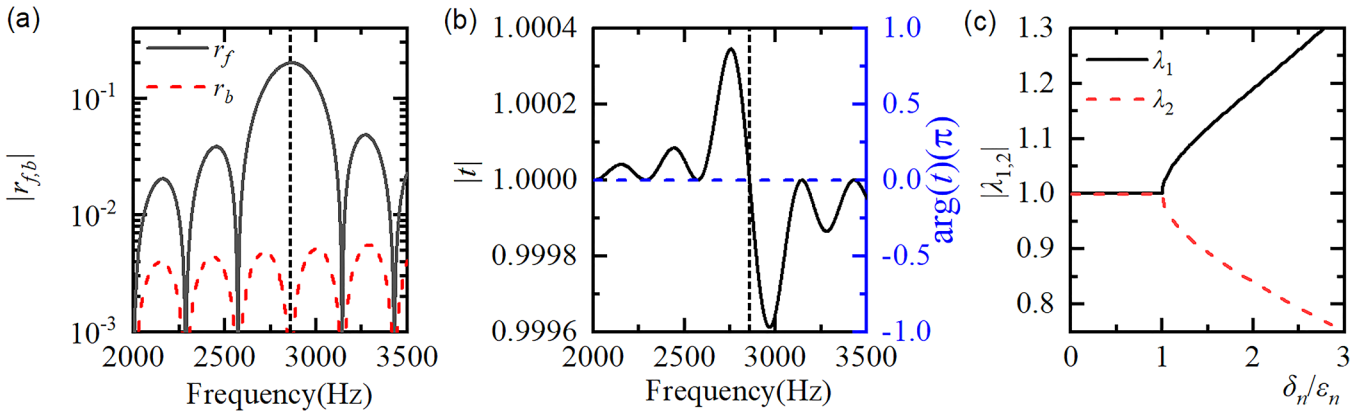

FIG. 2. Calculation results for the normal case: (a) amplitudes of the reflection coefficients and (b) amplitude and phase of the transmission coefficient, each as a function of frequency; (c) absolute value of the eigenvalues of the scattering matrix as a function of the imaginary-to-real-part ratio.

a strong reflection in the forward direction together with vanishing reflection in the backward direction would be observed. However, Figs. 3(a) and 3(b) show that the actual reflectionless direction reverses, that is, the PT-symmetric medium now becomes invisible from the forward direction ($|r_f| = 0$, $|t| = 1$, and $|\phi_t| = 0$). An EP can still be found at $\delta/\varepsilon = 1$ in Fig. 3(c), but in this case, is a result of vanishing r_f.

In case II, the PT-symmetric refractive index modulation is realized by tuning κ and ρ simultaneously (Table II). The calculation results are given in Figs. 3(d)–3(f), where the unidirectional invisibility and the related EP disappear. Instead, the bi-directional reflection exists at the first Bragg frequency.

B. Acoustic impedance

To understand the results of cases I and II, we carry out an intuitive analysis by considering the interference of backscattering waves. As shown in Fig. 4, r denotes the reflection coefficient at a specific interface, in which the subscript represents the interface between two adjacent layers. N is the total number of unit cells. k and Z represent the wavenumber and acoustic impedance with their subscript denoting the corresponding layer. Δk_Y and ΔZ_Y are defined as

$$\Delta k_Y = k_Y - k_0$$

TABLE II. Parameter distributions of cases I and II.

Component		A	B	C	D
Case I	ρ	ρ_0	$\rho_0(1-\varepsilon+\delta i)^2$	ρ_0	$\rho_0(1+\varepsilon-\delta i)^2$
	κ	$\frac{\kappa_0}{(1+\varepsilon+\delta i)^2}$	κ_0	$\frac{\kappa_0}{(1-\varepsilon-\delta i)^2}$	κ_0
Case II	ρ	$\rho_0(1+\varepsilon+\delta i)$	$\rho_0(1+\varepsilon+\delta i)$	$\rho_0(1-\varepsilon-\delta i)$	$\rho_0(1-\varepsilon-\delta i)$
	κ	κ_0	$\frac{\kappa_0(1+\varepsilon+\delta i)}{1-\varepsilon+\delta i}$	κ_0	$\frac{\kappa_0(1-\varepsilon-\delta i)}{1+\varepsilon-\delta i}$
	n	$n_0(1+\varepsilon+\delta i)$	$n_0(1-\varepsilon+\delta i)$	$n_0(1-\varepsilon-\delta i)$	$n_0(1+\varepsilon-\delta i)$

and

$$\Delta Z_Y = Z_Y - Z_0,$$

where Y can be A, B, C, or D.

We take interface BC in the leftmost unit cell as an example to analyze the reflected wave from an interface. Considering the transmission through interfaces 0A and AB and the phase delays in layers A and B, a unitary incident wave arriving at interface BC is formulated as

$$p_i|_{x=\frac{T}{2}} = t_{0A}t_{AB}e^{-i(k_0+\Delta k_A)\frac{mT}{2}}e^{-i(k_0+\Delta k_B)\frac{(1-m)T}{2}}. \tag{9}$$

The transmission coefficients at interfaces 0A and AB, t_{0A} and t_{AB}, are expressed by acoustic impedances as $t_{0A} = 2(Z_0 + \Delta Z_A)/(2Z_0 + \Delta Z_A)$ and $t_{AB} = 2(Z_0 + \Delta Z_B)/(2Z_0 + \Delta Z_A + \Delta Z_B)$. The reflected wave at interface BC is written as

$$p_r|_{x=\frac{T}{2}} = p_i|_{x=\frac{T}{2}}r_{BC}, \tag{10}$$

with reflection coefficient at interface BC being expressed as $r_{BC} = (\Delta Z_C - \Delta Z_B)/(2Z_0 + \Delta Z_B + \Delta Z_C)$. Again, considering the transmission and phase delays, the reflected wave traveling back to interface 0A reads as

$$p_r|_{x=0} = p_r|_{x=\frac{T}{2}}t_{BA}t_{A0}e^{-i(k_0+\Delta k_B)\frac{(1-m)T}{2}}e^{-i(k_0+\Delta k_A)\frac{mT}{2}}, \tag{11a}$$

where the transmission coefficients at interfaces BA and A0, t_{BA} and t_{A0}, are expressed as $t_{BA} = 2(Z_0 + \Delta Z_A)/(2Z_0 + \Delta Z_A + \Delta Z_B)$ and $t_{A0} = 2Z_0/(2Z_0 + \Delta Z_A)$. For small-amplitude modulation ($|\Delta k| \ll k_0$ and $|\Delta Z| \ll Z_0$), $p_r|_{x=0}$ can be simplified after ignoring

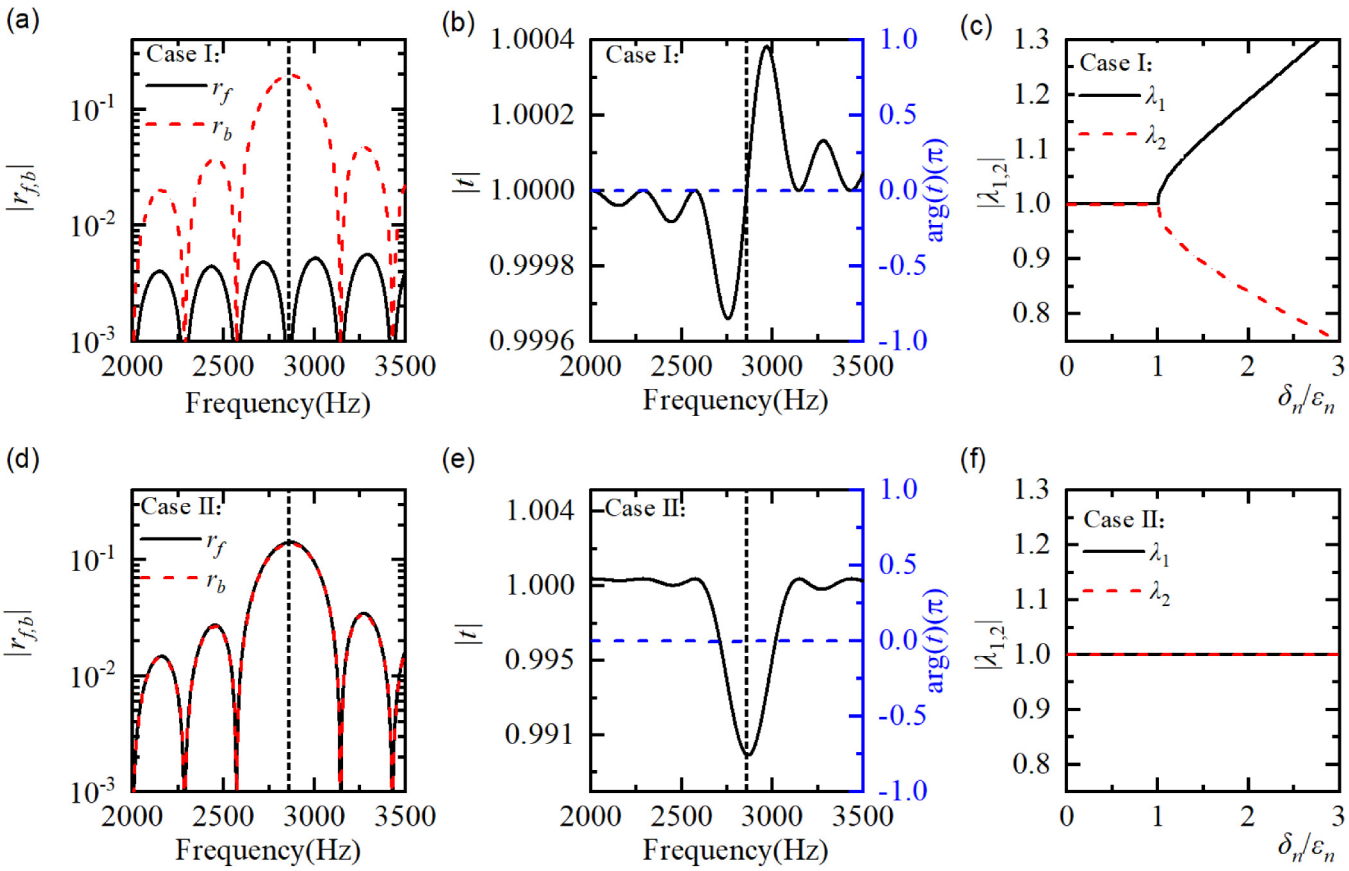

FIG. 3. Calculation results for case I and case II: [(a) and (d)] amplitudes of the reflection coefficients and [(b) and (e)] amplitude and phase of the transmission coefficient, each as a function of frequency; [(c) and (f)] absolute value of the eigenvalues of the scattering matrix as a function of the imaginary-to-real-part ratio.

the higher-order infinitesimals in the form

$$p_r|_{x=0} = r_{\mathrm{BC}} e^{-ik_0 T}, \tag{11b}$$

where r_{BC} is approximated as $\frac{\Delta Z_{\mathrm{C}} - \Delta Z_{\mathrm{B}}}{2Z_0}$. Notably, only the modulation on acoustic impedance exists in the expression of the reflected wave after the above simplification.

The reflected waves from other interfaces can be obtained in a similar way. The overall reflection coefficients from both sides can be approximated as the superposition of all the reflected waves,

$$\begin{aligned} r_f = {} & r_{0\mathrm{A}} + r_{\mathrm{AB}} e^{-2iA\times\frac{m}{2}} + r_{\mathrm{BC}} e^{-2iA\times\frac{1}{2}} + r_{\mathrm{CD}} e^{-2iA\times\left[\frac{1}{2}+\frac{1}{2}(1-m)\right]} \\ & + \left(\sum_{q=1}^{N-1} r_{\mathrm{DA}} e^{-2iAq} + r_{\mathrm{AB}} e^{-2iA\left(q+\frac{m}{2}\right)} + r_{\mathrm{BC}} e^{-2iA\left(q+\frac{1}{2}\right)} \right. \\ & \left. + r_{\mathrm{CD}} e^{-2iA\left[q+\frac{1}{2}+\frac{1}{2}(1-m)\right]} \right) + r_{\mathrm{D0}} e^{-2iAN} \end{aligned} \tag{12a}$$

and

$$\begin{aligned} r_b = {} & r_{\mathrm{A0}} e^{-2iAN} + r_{\mathrm{BA}} e^{-2iA\left(N-\frac{m}{2}\right)} + r_{\mathrm{CB}} e^{-2iA\left(N-\frac{1}{2}\right)} \\ & + r_{\mathrm{DC}} e^{-2iA\left[N-\frac{1}{2}-\frac{1}{2}(1-m)\right]} + \left(\sum_{q=0}^{N-2} r_{\mathrm{AD}} e^{-2iA(q+1)} \right. \\ & \left. + r_{\mathrm{BA}} e^{-2iA\left[q+\frac{1}{2}+\frac{1}{2}(1-m)\right]} + r_{\mathrm{CB}} e^{-2iA\left(q+\frac{1}{2}\right)} + r_{\mathrm{DC}} e^{-2iA\left(q+\frac{m}{2}\right)} \right) + r_{\mathrm{0D}}, \end{aligned} \tag{12b}$$

in which $A = k_0 T$, and $k_0 T = s\pi$ ($s \in Z^+$) denotes the sth order Bragg frequency. Each term of the right-hand side of Eq. (12) exactly represents the reflection from one interface. When $m = 0.5$ and $A = \pi$, the reflection coefficients can be written as

$$\begin{aligned} r_f = {} & r_{0\mathrm{A}} - i r_{\mathrm{AB}} - r_{\mathrm{BC}} + i r_{\mathrm{CD}} \\ & + \left(\sum_{q=1}^{N-1} r_{\mathrm{DA}} - i r_{\mathrm{AB}} - r_{\mathrm{BC}} + i r_{\mathrm{CD}} \right) + r_{\mathrm{D0}} \end{aligned} \tag{13a}$$

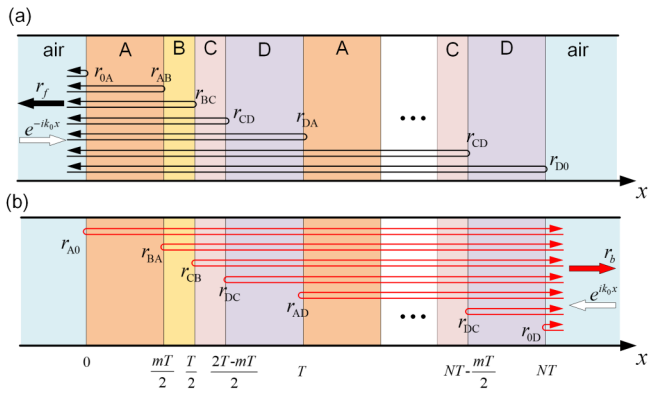

FIG. 4. Superposition of reflections from interfaces in the case of (a) forward and (b) backward incidence.

and

$$r_b = r_{A0} + ir_{BA} - r_{CB} - ir_{DC} + \left(\sum_{q=0}^{N-2} r_{AD} + ir_{BA} - r_{CB} - ir_{DC}\right) + r_{0D}. \quad (13b)$$

For the above normal case, after substituting the parameters into Eqs. (13a) and (13b), r_f and r_b can be obtained as $2\mathrm{Ni}(\varepsilon+\delta)$ and $2\mathrm{Ni}(\varepsilon-\delta)$, respectively. When $\varepsilon=\delta$, the reflected waves for forward incidence are in-phase, thereby leading to constructive interferences and strong reflection. By contrast, for backward incidence, these reflections are out-of-phase, resulting in complete destructive interferences and vanishing reflection.

In case I, r_f and r_b are expressed as $2N(\delta-\varepsilon)$ and $2N(\delta+\varepsilon)$. When $\varepsilon=\delta$, the directions of constructive and destructive interference reverse compared with the normal case, and the reflectionless direction reverses accordingly. In case II, the two terms are derived as

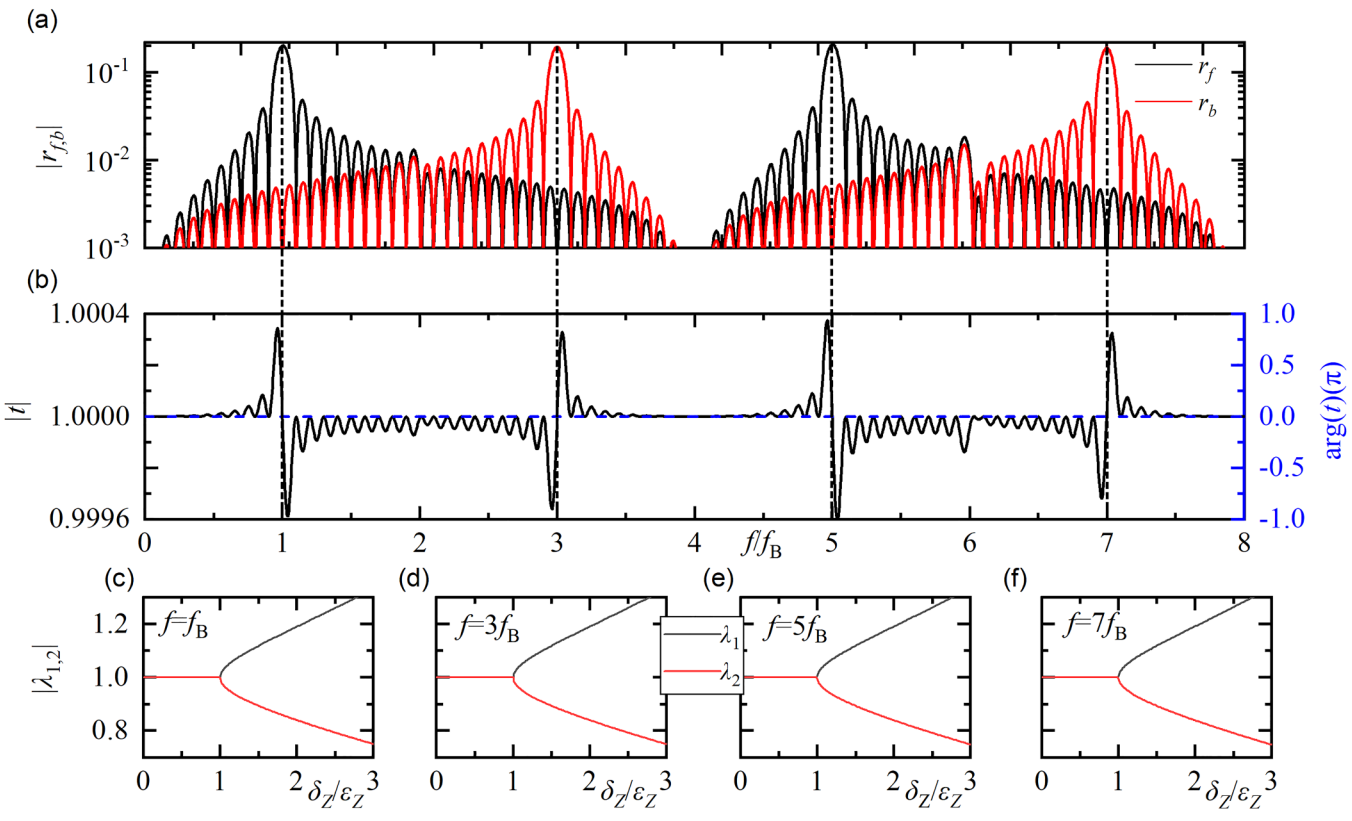

FIG. 5. Broadband scattering properties of the PT-symmetric multilayered medium for $\varepsilon_Z=\delta_Z$ and $m=0.5$. (a) Amplitudes of the reflection coefficients. (b) Amplitude and phase of the transmission coefficient.

$2N\varepsilon(1-i)$ and $2N\varepsilon(-1-i)$ with the same non-zero amplitudes, thereby leading to the symmetric bi-directional reflection.

From the above analysis, for small-amplitude modulation with fixed modulation period and total length, the acoustic impedance exclusively determines the scattering property of the PT-symmetric system. Therefore, we conclude that the modulation on acoustic impedance should be a more appropriate way to describe PT-symmetric scattering systems and characterize the existence of EPs.

V. UNIDIRECTIONAL INVISIBILITY IN THE CASES OF UNEQUAL MODULATION AND RECTANGULAR REAL-PART MODULATION

The unidirectional invisibility supported by PT-symmetric multilayered structures is usually considered at the first-order Bragg frequency. Moreover, the real and imaginary part modulations are designed to have the same amplitude and ideal square-wave form (equal positive and negative half-cycles). These reduce the flexibilities of achieving unidirectional invisibility and constructing artificial structures. In this section, we investigate the EPs of the scattering matrix in a broad band and explore the possibilities of relaxing the restrictions on the PT-symmetric modulation.

A. Condition of EP

The modulation on acoustic impedance is adopted in the following discussion, with its real and imaginary amplitudes being ε_Z and δ_Z. Then, Eqs. (12a) and (12b) are arranged and rewritten as

$$r_f \approx \begin{cases} ie^{-iA}\{-\delta_Z+\delta_Z\cos A+\varepsilon_Z\sin A-2\varepsilon_Z\sin[(1-m)A]\}, & N=1,\\ 2ie^{-iNA}\sum_{j=1}^{q}\cos[(2j-1)A]\{-\delta_Z+\delta_Z\cos A+\varepsilon_Z\sin A-2\varepsilon_Z\sin[(1-m)A]\}, & N=2q,\\ ie^{-iNA}(1+2\sum_{j=1}^{q}\cos 2jA)\{-\delta_Z+\delta_Z\cos A+\varepsilon_Z\sin A-2\varepsilon_Z\sin[(1-m)A]\}, & N=2q+1, \end{cases} \tag{14a}$$

$$r_b \approx \begin{cases} ie^{-iA}\{\delta_Z-\delta_Z\cos A+\varepsilon_Z\sin A-2\varepsilon_Z\sin[(1-m)A]\}, & N=1,\\ 2ie^{-iNA}\sum_{j=1}^{q}\cos[(2j-1)A]\{\delta_Z-\delta_Z\cos A+\varepsilon_Z\sin A-2\varepsilon_Z\sin[(1-m)A]\}, & N=2q,\\ ie^{-iNA}(1+2\sum_{j=1}^{q}\cos 2jA)\{\delta_Z-\delta_Z\cos A+\varepsilon_Z\sin A-2\varepsilon_Z\sin[(1-m)A]\}, & N=2q+1, \end{cases} \tag{14b}$$

where $q \in Z^+$. According to the above expressions of reflection coefficients, the condition of EP is concluded as

$$\begin{cases} \delta_Z-\delta_Z\cos A=\varepsilon_Z\sin A-2\varepsilon_Z\sin[(1-m)A] & (r_f=0 \text{ and } r_b\neq 0),\\ -\delta_Z+\delta_Z\cos A=\varepsilon_Z\sin A-2\varepsilon_Z\sin[(1-m)A] & (r_b=0 \text{ and } r_f\neq 0). \end{cases} \tag{15}$$

B. Unidirectional invisibility at higher-order Bragg frequencies

We first examine the broadband scattering properties of a balanced square-wave modulation on the acoustic impedance, that is, $\varepsilon_Z=\delta_Z$ and $m=0.5$. The condition of EP becomes $A=2s\pi+\pi$ (s is an even number for invisibility in the backward direction, whereas an odd number for the forward one). This condition is further confirmed by numerical calculation with the parameters being the same as the normal case. As shown in Figs. 5(a) and 5(b), unidirectional invisibility in the backward (forward) direction, where $r_b=0$, $r_f\neq 0$, and $t=1$ ($r_f=0$, $r_b\neq 0$, and $t=1$), takes place at the first- (three) and five- (seven) order Bragg frequencies.

From the viewpoint of momentum space, the Fourier expansion of the complex square wave contains odd-number-fold $2k_B$ that satisfies the wave-vector matching condition for incident acoustic wave from only one direction. For example, when the system operates at the third-order Bragg frequency, the PT-symmetric medium offers a unidirectional modulation vector $\boldsymbol{q}=6k_B\boldsymbol{x}/x$. The wave-vector matching condition, $\boldsymbol{k}_r=\boldsymbol{q}+\boldsymbol{k}_i$ ($\boldsymbol{k}_i$ and $\boldsymbol{k}_r$ are incident and reflected wave vectors whose magnitudes are $3k_B$ and opposite with each other), is only satisfied for backward incidence, thereby leading to the invisibility from the forward direction.

C. Unequal amplitudes of real and imaginary part modulations

In practice, obtaining balanced real and imaginary part modulations through artificial structures may be difficult. Actually, even in the case of unequal real and imaginary part modulations ($\varepsilon_Z\neq\delta_Z$), the unidirectional invisibility and EP can still exist. Reconsidering the condition of EP [Eq. (15)], and when $m=0.5$,

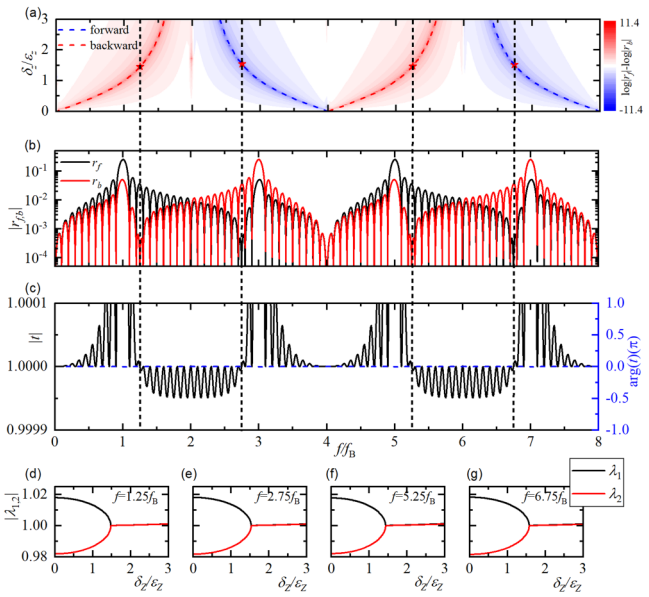

FIG. 6. Broadband scattering properties of the PT-symmetric multilayered medium for $\varepsilon_Z \neq \delta_Z$ and $m = 0.5$. (a) Plot of Eq. (16) and the ratio of the forward and backward reflection amplitudes, each as a function of the amplitude modulation ratio and frequency. The red stars denote four unidirectional invisibility points when $\delta_Z/\varepsilon_Z = 1.497$. (b) Amplitudes of the reflection coefficients. (c) Amplitude and phase of the transmission coefficient. [(d)–(g)] Absolute value of the eigenvalues of the scattering matrix.

the formula is simplified as

$$\begin{cases} \delta_Z/\varepsilon_Z = -\tan\left(\dfrac{A}{4}\right) & (r_f = 0 \text{ and } r_b \neq 0), \\ \delta_Z/\varepsilon_Z = \tan\left(\dfrac{A}{4}\right) & (r_b = 0 \text{ and } r_f \neq 0), \end{cases} \tag{16}$$

where A can be substituted by $\pi f/f_B$. The above condition indicates that achieving EP at multi-frequencies is possible as long as the value of δ_Z/ε_Z satisfies Eq. (16), as shown in Fig. 6(a). The result is further verified through a calculation similar to that of Sec. IV A but with different δ_Z/ε_Z values. Figure 6(a) shows the contrast (in logarithmic scale) between the forward and backward reflection coefficients, $\log|r_f| - \log|r_b|$, in which extremely asymmetric reflection can be observed over the spectrum for a series of specific δ_Z/ε_Z values. To further confirm that the strong asymmetry in reflection indeed corresponds to the emergence of unidirectional invisibility, we take the modulation amplitude ratio of 1.497 as an example and examine the amplitude and phase responses at four frequencies, $1.25f_B$, $2.75f_B$, $5.25f_B$, and $6.75f_B$ [as marked by the red stars in Fig. 6(a)]. It is seen that invisibility in the forward (backward) direction occurs at $2.75f_B$ and $6.75f_B$ ($1.25f_B$ and $5.25f_B$), each signifying an EP in the parameter space as shown in Figs. 6(d)–6(g).

D. Rectangular real-part modulation

The unequal amplitudes of real and imaginary part modulations make unidirectional invisibility deviate from the Bragg

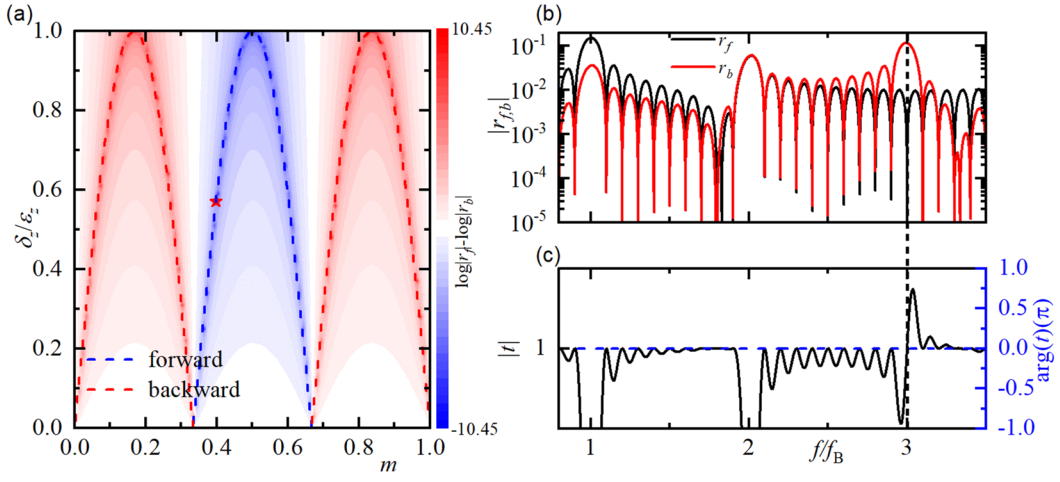

FIG. 7. Broadband scattering properties of the PT-symmetric multilayered medium for $\varepsilon_Z \neq \delta_Z$ and $m \neq 0.5$. (a) Plot of Eq. (17) and the ratio of the forward and backward reflection amplitudes, each as a function of the amplitude modulation ratio and duty ratio of real-part modulation. The red star denotes the selected unidirectional invisibility point when $m = 0.4$ and $\delta_Z/\varepsilon_Z = 0.588$. (b) Amplitudes of the reflection coefficients. (c) Amplitude and phase of the transmission coefficient.

frequencies as discussed in Sec. V C. In this section, an additional variable, that is, the duty ratio of the negative real part modulation m, is introduced to redirect the working frequency back to the Bragg resonance frequency. We select the working frequency as $3f_B$, and the condition of EP is given by

$$\begin{cases} \delta_Z/\varepsilon_Z = -\sin[3\pi(1-m)] & (r_f = 0 \text{ and } r_b \neq 0), \\ \delta_Z/\varepsilon_Z = \sin[3\pi(1-m)] & (r_b = 0 \text{ and } r_f \neq 0), \end{cases} \tag{17}$$

which is plotted in Fig. 7(a). In addition, Fig. 7(a) shows the contrast between forward and backward reflection coefficients when δ_Z/ε_Z and m change from 0 to 1, which confirms the results obtained in Eq. (17). We further select a point ($m = 0.4$, $\delta_Z/\varepsilon_Z = 0.588$) within the parameter region showing a large reflection asymmetry to further investigate its reflection and transmission coefficients over the spectrum. As shown in Figs. 7(b) and 7(c), invisibility in the forward direction can be observed at $3f_B$. That is, by adjusting δ_Z/ε_Z and m, the unidirectional invisibility can be well tuned back to the Bragg resonance.

Notably, the results are obtained in the small-amplitude modulation regime. Owing to this assumption, the total reflection can be treated as the superposition of the reflections from all the interfaces, allowing us to derive an explicit expression of the condition of EPs. Beyond this regime, EPs can also be achieved, but an explicit expression is not available anymore and numerical calculations need to be performed to find the locations of EPs in the parameter space.[13,26]

VI. CONCLUSION

To conclude, we have revealed that acoustic impedance instead of refractive index is the key parameter that governs the scattering behavior and the occurrence of unidirectional invisibility or reflectionlessness in PT-symmetric media with small-amplitude modulation. In addition, the broadband scattering properties and the distribution of EP within the spectrum are fully investigated, during which more flexible modulation approaches are discussed. This work could benefit the design and practical realization of PT-symmetric scattering systems supporting unidirectional invisibility or reflectionlessness. Our result may also be applied to other non-Hermitian systems under small-amplitude modulation not limited to the PT-symmetric ones.

ACKNOWLEDGMENTS

This work was supported by the Research Grants Council of Hong Kong SAR (Grant Nos. C6013-18G and PolyU 152119/18E) and the National Natural Science Foundation of China (Grant No.11774297).

DATA AVAILABILITY

The data that support the findings of this study are available from the corresponding author upon reasonable request.

REFERENCES

[1]C. M. Bender and S. Boettcher, Phys. Rev. Lett. **80**(24), 5243–5246 (1998).
[2]S. K. Ozdemir, S. Rotter, F. Nori, and L. Yang, Nat. Mater. **18**(8), 783–798 (2019).
[3]M.-A. Miri and A. Alù, Science **363**(6422), eaar7709 (2019).
[4]L. Feng, R. El-Ganainy, and L. Ge, Nat. Photonics **11**(12), 752–762 (2017).
[5]S. K. Gupta, Y. Zou, X. Y. Zhu, M. H. Lu, L. J. Zhang, X. P. Liu, and Y. F. Chen, Adv. Mater. **32**(27), e1903639 (2020).
[6]R. El-Ganainy, K. G. Makris, M. Khajavikhan, Z. H. Musslimani, S. Rotter, and D. N. Christodoulides, Nat. Phys. **14**(1), 11–19 (2018).
[7]H. Zhao and L. Feng, Natl. Sci. Rev. **5**(2), 183–199 (2018).
[8]S. Longhi, J. Phys. A: Math. Theor. **44**(48), 485302 (2011).
[9]Z. Lin, H. Ramezani, T. Eichelkraut, T. Kottos, H. Cao, and D. N. Christodoulides, Phys. Rev. Lett. **106**(21), 213901 (2011).
[10]L. Feng, Y. L. Xu, W. S. Fegadolli, M. H. Lu, J. E. Oliveira, V. R. Almeida, Y. F. Chen, and A. Scherer, Nat. Mater. **12**(2), 108–113 (2013).
[11]X. Zhu, H. Ramezani, C. Shi, J. Zhu, and X. Zhang, Phys. Rev. X **4**(3), 031042 (2014).
[12]L. Ge, Y. D. Chong, and A. D. Stone, Phys. Rev. A **85**(2), 023802 (2012).
[13]R. Fleury, D. Sounas, and A. Alù, Nat. Commun. **6**(1), 5905 (2015).
[14]E. Rivet, A. Brandstötter, K. G. Makris, H. Lissek, S. Rotter, and R. Fleury, Nat. Phys. **14**(9), 942–947 (2018).
[15]Y. Auregan and V. Pagneux, Phys. Rev. Lett. **118**(17), 174301 (2017).
[16]W. Zhu, X. Fang, D. Li, Y. Sun, Y. Li, Y. Jing, and H. Chen, Phys. Rev. Lett. **121**(12), 124501 (2018).
[17]A. Merkel, V. Romero-García, J.-P. Groby, J. Li, and J. Christensen, Phys. Rev. B **98**(20), 201102 (2018).
[18]C. Shen, J. Li, X. Peng, and S. A. Cummer, Phys. Rev. Mater. **2**(12), 125203 (2018).
[19]V. Domínguez-Rocha, R. Thevamaran, F. M. Ellis, and T. Kottos, Phys. Rev. Appl. **13**(1), 014060 (2020).
[20]T. Liu, X. Zhu, F. Chen, S. Liang, and J. Zhu, Phys. Rev. Lett. **120**(12), 124502 (2018).
[21]Y. Yang, H. Jia, Y. Bi, H. Zhao, and J. Yang, Phys. Rev. Appl. **12**(3), 034040 (2019).
[22]H.-Z. Chen, T. Liu, H.-Y. Luan, R.-J. Liu, X.-Y. Wang, X.-F. Zhu, Y.-B. Li, Z.-M. Gu, S.-J. Liang, H. Gao, L. Lu, L. Ge, S. Zhang, J. Zhu, and R.-M. Ma, Nat. Phys. **16**(5), 571–578 (2020).
[23]Y. Yang, H. Jia, S. Wang, P. Zhang, and J. Yang, Appl. Phys. Lett. **116**(21), 213501 (2020).
[24]Y. Yang, H. Jia, and J. Yang, J. Acoust. Soc. Am. **148**(1), 33–43 (2020).
[25]T. Liu, G. Ma, S. Liang, H. Gao, Z. Gu, S. An, and J. Zhu, Phys. Rev. B **102**(1), 014306 (2020).
[26]C. Shi, M. Dubois, Y. Chen, L. Cheng, H. Ramezani, Y. Wang, and X. Zhang, Nat. Commun. **7**(1), 11110 (2016).
[27]J. Lan, L. Wang, X. Zhang, M. Lu, and X. Liu, Phys. Rev. Appl. **13**(3), 034047 (2020).
[28]B. J. Tester, J. Sound Vib. **27**(4), 477–513 (1973).
[29]A. H. Nayfeh, J. E. Kaiser, and D. P. Telionis, AIAA J. **13**(2), 130–153 (1975).
[30]C. Cho, X. Wen, N. Park, and J. Li, Nat. Commun. **11**(1), 251 (2020).
[31]B. H. Song and J. S. Bolton, J. Acoust. Soc. Am. **107**(3), 1131–1152 (2000).